

# Communicating via ignorance

K. Goswami,\* J. Romero, and A. G. White

Centre for Engineered Quantum Systems, School of Mathematics and Physics, University of Queensland, QLD 4072 Australia  
(Dated: July 24, 2018)

Communication through a sequence of two identical, noisy, depolarising channels is impossible in conventional information theory. Surprisingly, communication becomes possible if the depolarising channels are within a quantum switch, where the order of the channels is in a quantum superposition. Here, we experimentally demonstrate this counterintuitive result in a quantum switch that uses polarisation to coherently control the order of two depolarising channels acting on the transverse spatial mode of a photon. We send  $(3.41 \pm 0.15) \times 10^{-2}$  bits of information through two fully depolarising channels that are in an indefinite causal order.

Since noise is ubiquitous, communication protocols aim to optimise the amount of information that can be sent through a channel with a given amount of noise: in the limit of a completely noisy channel no information can be transmitted. To date, quantum information has extended Shannon's original information theory by considering situations where channels remain classical but information carriers are quantum [1–4]. Recently it has been shown how to form quantum channels where there is superpositions of the causal order in which gates or channels are applied [5–8]. This leads to a quantum advantage in communication [9] and computation [10].

Here we show that it is possible to send information through completely noisy channels—which is classically impossible—if we are ignorant of the order that we go through the channels, technically the order of the two channels is indefinite. We use a quantum switch [5, 7, 8, 10]: in our implementation, the control qubit is photonic polarisation which controls the order of the two quantum channels for the target qubit, which is the photonic transverse spatial mode [8].

Figure 1 outlines our protocol, following the proposal of [9]. The operations  $\mathcal{N}^q$  and  $\mathcal{M}^q$  are noisy depolarising channels, where  $q$  denotes the strength of depolarisation in the channel:  $q=0$  signifies a clean channel, i.e. no depolarisation. The order of the channels is selected by a control qubit in a quantum switch,  $\mathfrak{s}[\mathcal{N}^q, \mathcal{M}^q]$ . If the control is off,  $|0\rangle_c$ , then  $\mathcal{N}^q \circ \mathcal{M}^q$ , i.e.  $\mathcal{N}^q$  is before  $\mathcal{M}^q$ . If the control is on,  $|1\rangle_c$ , then  $\mathcal{M}^q \circ \mathcal{N}^q$ . In either case no communication is possible via the target qubit since the Holevo capacity—the maximum amount of classical information that can be transferred through any channel [9, 11]—is  $\chi=0$ . However, if the control polarisation is diagonal,  $|D\rangle_c = (|0\rangle + |1\rangle)_c / \sqrt{2}$ , the channels for the target qubit are applied in superposition, i.e.  $\mathcal{N}^q$  and  $\mathcal{M}^q$  have indefinite causal order, and  $\chi > 0$ . Specifically the Holevo capacity of two noisy channels in a quantum switch is, [9]

$$\chi(\mathfrak{s}[\mathcal{N}^q, \mathcal{M}^q]) = 1 + H(\tilde{\rho}_c) - H^{\min}(\mathfrak{s}[\mathcal{N}^q, \mathcal{M}^q]), \quad (1)$$

where  $H^{\min}(\mathfrak{s}[\mathcal{N}^q, \mathcal{M}^q])$  is the minimum entropy of the two-qubit output of the quantum switch, and  $H(\tilde{\rho}_c)$  is

the Von-Neumann entropy of the output control qubit  $\tilde{\rho}_c$ , after tracing out the target qubit from the output state.

Quantifying the Holevo capacity requires measuring the output control  $\tilde{\rho}_c$ . Since our control qubit is polarisation, we express the output control in terms of the Stokes vector  $(S_1, S_2, S_3)$  [12]:

$$\tilde{\rho}_c = \frac{1}{2} \begin{pmatrix} 1+S_1 & S_2+iS_3 \\ S_2-iS_3 & 1-S_1 \end{pmatrix} \quad (2)$$

Now consider the target qubit. We model a depolarising channel as a linear combination of all three Pauli errors and the identity operation, where:  $\sigma_1 \equiv x$  is a bit flip ( $\pi/2$  rotation of the spatial mode);  $\sigma_3 \equiv z$  is a phase flip ( $\pi$  rotation of the spatial mode);  $\sigma_2 \equiv y$  is a combination of bit flip and phase flip; and  $\sigma_0 \equiv i$ .

$$\mathcal{N}^q(\rho_t) = \sum_{i=0}^3 p_i \sigma_i \rho_t \sigma_i^\dagger \quad (3)$$

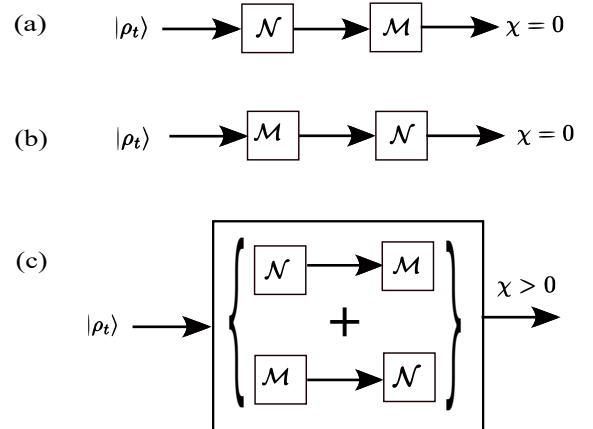


FIG. 1. Definite vs indefinite order of noisy channels.  $\mathcal{N}$  and  $\mathcal{M}$  are completely depolarising channels acting on the target  $|\rho_t\rangle$ . (a) When the control qubit is off,  $|\rho_c\rangle = |0\rangle$ , and the channels have a definite causal order  $\mathcal{N} \circ \mathcal{M}$ . The Holevo capacity, which is the maximum rate of information transfer, is  $\chi=0$ . (b) When the control qubit is on,  $|\rho_c\rangle = |1\rangle$ , the order is  $\mathcal{M} \circ \mathcal{N}$  and again  $\chi=0$ . (c) When the control is in a superposition,  $|\rho_c\rangle = (|0\rangle + |1\rangle)/\sqrt{2}$ , the channels have an indefinite causal order and the Holevo capacity is non-zero.

\* k.goswami@uq.edu.au

The coefficients  $\{p_i\}$  are a function of  $q$ , defined as  $p_0=1-3q/4$ ,  $p_1=p_2=p_3=q/4$ .

With an input control state  $\rho_c=|\rho_c\rangle\langle\rho_c|$ , where  $|\rho_c\rangle=\sqrt{\gamma}|0\rangle+\sqrt{1-\gamma}|1\rangle$  and  $\gamma\in\mathbb{R}$ , a switch between two channels  $\mathcal{N}^q$  and  $\mathcal{M}^q$  operates on the control and target qubits to give the output:

$$\begin{aligned} \rho_{out} &= \mathfrak{s}[\mathcal{N}^q, \mathcal{M}^q] (\rho_c \otimes \rho_t) = \\ &\sum_{i,j} p_i p_j (\gamma |0\rangle\langle 0|_c \otimes \sigma_i \sigma_j \rho_t \sigma_i^\dagger \sigma_j^\dagger \\ &\quad + (1-\gamma) |1\rangle\langle 1|_c \otimes \sigma_j \sigma_i \rho_t \sigma_i^\dagger \sigma_j^\dagger \\ &\quad + (1-\gamma) |1\rangle\langle 1|_c \otimes \sigma_j \sigma_i \rho_t \sigma_i^\dagger \sigma_j^\dagger \\ &\quad + \sqrt{\gamma(1-\gamma)} |0\rangle\langle 1|_c \otimes \sigma_i \sigma_j \rho_t \sigma_i^\dagger \sigma_j^\dagger \\ &\quad + \sqrt{\gamma(1-\gamma)} |1\rangle\langle 0|_c \otimes \sigma_j \sigma_i \rho_t \sigma_i^\dagger \sigma_j^\dagger) \\ &= \sum_{i,j} p_i p_j \mathfrak{s}[\sigma_i, \sigma_j] (\rho_c \otimes \rho_t) \end{aligned} \quad (4)$$

Note that this equation shows that the action of depolarising channels in a quantum switch can be considered as a statistical mixture of the action of the quantum switch with unitaries  $\sigma_i$  and  $\sigma_j$ .

Tracing out the target qubit from the output of a quantum switch having two depolarising channels of strength  $q$  given in (4), the Stokes parameters of the output control  $\tilde{\rho}_c$  are given by:

$$S_1=S_1^{in}, \quad S_3=S_3^{in}, \quad \text{and} \quad S_2=(1-3q^2/4). \quad (5)$$

Here  $S_1^{in}$  and  $S_3^{in}$  are Stokes parameters for the input control  $\rho_c$ . We see that that the quantum switch affects only the  $S_2$  component of the control qubit. Accordingly, the Holevo capacity is maximum when  $\gamma=1/2$ , i.e. for input control  $|\rho_c\rangle=(|0\rangle+|1\rangle)/\sqrt{2}$ , where  $S_2^{in}=1$  and  $S_1^{in}=S_3^{in}=0$ .

We now show that to assess the action of the quantum switch,  $\mathfrak{s}[\mathcal{N}^q, \mathcal{M}^q]$ , we need only to consider its effect on the  $S_2$  component of the control,

$$\begin{aligned} S_2(\mathfrak{s}[\mathcal{N}^q, \mathcal{M}^q]) &= \text{Tr} \{ (X \otimes \sigma_0) \cdot \mathfrak{s}[\mathcal{N}^q, \mathcal{M}^q] \} \\ &= \sum_{i,j} p_i p_j \text{Tr} \{ (X \otimes \sigma_0) \cdot \mathfrak{s}[\sigma_i, \sigma_j] \} \\ &= \sum_{i,j} p_i p_j S_2(\mathfrak{s}[\sigma_i, \sigma_j]) \end{aligned} \quad (6)$$

That is, measuring the control output in the Pauli  $X$  basis—the diagonal/antidiagonal polarisation basis—for each combination of Pauli operations on the target,  $S_2(\mathfrak{s}[\sigma_i, \sigma_j])$ , enables us to measure the operation of a switch with depolarising channels  $\mathcal{N}^q, \mathcal{M}^q$  on the  $S_2$  parameter.

Equation (5) gives us  $\tilde{\rho}_c$ , and thus from equation (1) the Von Neumann entropy  $H(\tilde{\rho}_c)$ , which is necessary to obtain the Holevo capacity .

$\sigma_i$	$\sigma_j$	$\tilde{\rho}_t$	$\tilde{\rho}_c$	$S_2(\sigma_i, \sigma_j)^{\text{theor.}}$	$S_2(\sigma_i, \sigma_j)^{\text{exp.}}$
$\sigma_0$	$\sigma_0$	$ 1\rangle$	D	1	$0.8547 \pm 0.0006$
	$\sigma_1$	$ 0\rangle$	D	1	$0.8718 \pm 0.0005$
	$\sigma_2$	$-i 0\rangle$	D	1	$0.8792 \pm 0.0005$
$\sigma_1$	$\sigma_3$	$- 1\rangle$	D	1	$0.8823 \pm 0.0005$
	$\sigma_0$	$ 0\rangle$	D	1	$0.8459 \pm 0.0006$
	$\sigma_1$	$ 1\rangle$	D	1	$0.8439 \pm 0.0007$
$\sigma_2$	$\sigma_2$	$-i 1\rangle$	A	-1	$-0.8434 \pm 0.0006$
	$\sigma_3$	$- 0\rangle$	A	-1	$-0.8540 \pm 0.0007$
	$\sigma_0$	$-i 0\rangle$	D	1	$0.8473 \pm 0.0007$
$\sigma_3$	$\sigma_1$	$i 1\rangle$	A	-1	$-0.8600 \pm 0.0005$
	$\sigma_2$	$ 1\rangle$	D	1	$0.8447 \pm 0.0006$
	$\sigma_3$	$i 0\rangle$	A	-1	$-0.8278 \pm 0.0008$
$\sigma_3$	$\sigma_0$	$- 1\rangle$	D	1	$0.8316 \pm 0.0006$
	$\sigma_1$	$ 0\rangle$	A	-1	$-0.8228 \pm 0.0006$
	$\sigma_2$	$-i 0\rangle$	A	-1	$-0.8575 \pm 0.0006$
	$\sigma_3$	$ 1\rangle$	D	1	$0.8780 \pm 0.0005$

TABLE I. Data for the different combinations of unitary operations  $\sigma_i$  and  $\sigma_j$ .  $\tilde{\rho}_t$  and  $\tilde{\rho}_c$  are the output target and control state respectively.  $S_2(\sigma_i, \sigma_j)$  is the Stokes parameter of obtained by measuring polarisation of the control qubit in the diagonal/anti-diagonal basis after the unitaries  $\sigma_i$  and  $\sigma_j$ . We list both the theoretically expected values,  $S_2(\sigma_i, \sigma_j)^{\text{theor.}}$ , and the experimentally measured values,  $S_2(\sigma_i, \sigma_j)^{\text{exp.}}$ , of this Stokes parameter. Error bars ( $1\sigma$ ) were calculated by propagation of error on the individual Stokes parameter with Poissonian counting statistics.

The other quantity needed to evaluate (1) is the minimum entropy of the total output  $H^{\min}(\mathfrak{s}[\mathcal{N}^q, \mathcal{M}^q])$ . Again we use (4), and notice that pairwise combinations of  $\{\sigma_i\}$  operators either commute or anti-commute. Projecting the control qubit into the diagonal/antidiagonal basis thus results to a product state. Denoting the anti-commutator by  $\{\dots\}$  and the commutator by  $[\dots]$ , the output state is  $|+\rangle\langle +|_c \otimes \{\sigma_i, \sigma_j\} \rho_t \{\sigma_i, \sigma_j\}^\dagger$  for commuting operations or  $|-\rangle\langle -|_c \otimes [\sigma_i, \sigma_j] \rho_t [\sigma_i, \sigma_j]^\dagger$  for anti-commuting operations. The quantities  $|+\rangle\langle +|_c$  or  $|-\rangle\langle -|_c$  correspond to the Stokes parameter  $S_2(\mathfrak{s}[\sigma_i, \sigma_j])$ . For commuting operations, the theoretical Stokes parameter  $S_2(\mathfrak{s}[\sigma_i, \sigma_j])$  is 1 and for anti-commuting operations  $S_2(\mathfrak{s}[\sigma_i, \sigma_j])$  is  $-1$ .

In our experiment, the maximum measured rate at the control output is around 100,000 counts per second. We measure, over 10 s,  $S_2(\mathfrak{s}[\sigma_i, \sigma_j])$  for each pair  $\sigma_i, \sigma_j$ ; using equation (5) allows us to find each state  $\mathfrak{s}[\sigma_i, \sigma_j](\rho_c \otimes \rho_t)$ . Combining these as per equation (4) then yields the state  $\mathfrak{s}[\mathcal{N}^q, \mathcal{M}^q](\rho_c \otimes \rho_t)$ . Note that the value of  $q$  determines the weighting of that combination.

Table I summarises the results. The first two columns are the ideal settings for the target operations,  $\sigma_i, \sigma_j$ , the third and fourth columns are the ideal output transformations,  $\tilde{\rho}_t, \tilde{\rho}_c$ . Figure 2 shows the action of the transformations from column 3 on our choice of input target qubit. The last two columns are the ideal and measured values of the  $S_2$  parameter of the control output.

The uncertainty in each measurement,  $S_2(\sigma_i, \sigma_j)^{\text{exp.}}$ , is small, due to the large number of counts. Computer-controlled waveplates, with a settings uncertainty of  $\pm(2.5 \times 10^{-4})^\circ$ , are used to measure in the diagonal/anti-

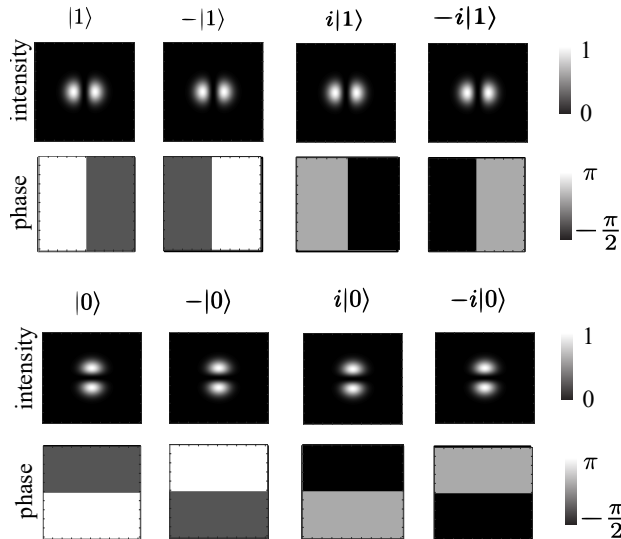


FIG. 2. Predicted spatial mode of target qubit outputs,  $\tilde{\rho}_t$ , after the Pauli operations  $\{\sigma_i, \sigma_j\}$  (see columns 1–3 of Table I). The input target qubit  $\rho_t$  is  $|1\rangle = \text{HG}_{10}$ .

diagonal basis. The value of  $S_2$  is limited by the non-ideal interferometric visibility in our switch: which is  $85.3 \pm 1.8\%$ . This is due to several factors: the unitary operations on the spatial mode are limited by the relatively coarse rotation accuracy of the inverting prisms,  $\pm 0.5^\circ$ ; further, each optical element is not perfectly flat, introducing wavefront distortions that limit the final visibility. Further details of the experimental setup we use to obtain  $S_2(\mathfrak{s}[\sigma_i, \sigma_j])$  can be found in the supplementary material and [8].

From these measurements we calculate  $H(\tilde{\rho}_c)$  and the minimum entropy  $H^{\min}(\mathfrak{s}[\mathcal{N}^q, \mathcal{M}^q])$  to evaluate the Holevo capacity  $\chi$  for different depolarising channel strengths, as described above. Figure 3 shows the logarithm of  $\chi$ , plotted against different depolarising strengths of the channel  $q$ . The red circles are our measured values; the orange shaded region is the predicted Holevo capacity for visibilities of  $85.3 \pm 1.8\%$ ; the black curve is the Holevo capacity for an ideal quantum switch. The blue curve is the ideal Holevo capacity for classical channels—i.e. two depolarising channels in some definite causal order—which decreases monotonically with increasing depolarising strength; in the limit of two fully depolarising channels,  $q = 1$ ,  $\chi = 0$  bits are transmitted. In this limit there is a clear advantage in using quantum channels: ideally  $4.88 \times 10^{-2}$  bits can be transmitted, we measure  $\chi = (3.41 \pm 0.15) \times 10^{-2}$  bits.

This nonzero Holevo capacity can be understood intuitively from Equation (4), which shows that the output of a quantum switch with two depolarising channels is a statistical mixture of the output of a quantum switch with different Pauli operations  $\{\sigma_i\}$ . Some of these Pauli operations anti-commute, hence superpositions of the order of anti-commuting Pauli operations—as is possible in a quantum switch—can preserve a finite amount of information in the target qubit. This explains the result of

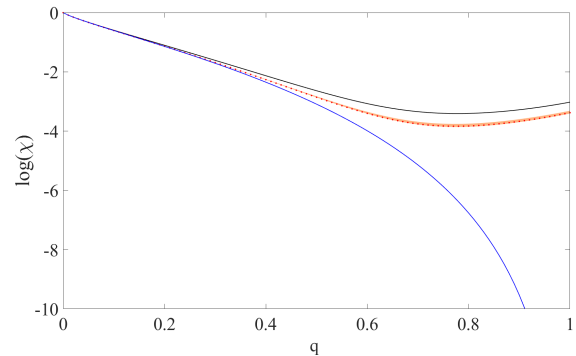


FIG. 3. Logarithm of Holevo capacity  $\chi$ , of two depolarising channels,  $\mathcal{N}^q$  and  $\mathcal{M}^q$  versus depolarising channel strength,  $q$ . The blue line is the predicted Holevo capacity for the classical case of definite order, Fig. 1(a,b). The black line is the predicted Holevo capacity for the quantum case of indefinite order, Fig. 1(c). The red dots are the measured values for Holevo capacity in our quantum switch; in excellent agreement with the predicted Holevo capacity for our experimental visibilities  $85.3 \pm 1.8\%$ , shown by the orange shaded area. Note that the minimum measured Holevo capacity of  $\chi < (2.15 \pm 0.15) \times 10^{-2}$  bits occurs at a depolarisation  $q = 0.78$ , and that higher capacity of  $\chi = (3.41 \pm 0.15) \times 10^{-2}$  bits occurs at full depolarisation,  $q = 1$ .

Reference [9]—which the authors highlighted as counter-intuitive—that the Holevo capacity decreases with increasing dimensionality of the target state. For qudits, the Holevo capacity will decrease since the proportion of generalised Pauli operators that anti-commute also decreases.

We experimentally confirm another striking prediction, which is that above some non-zero depolarisation strength the Holevo capacity will increase. In the ideal case, we see that Holevo capacity attains a minimum value of  $3.32 \times 10^{-2}$  bits at  $q = 0.7778$  and then the capacity increases to the limit of  $4.88 \times 10^{-2}$  bits at  $q = 1$ , in stark contrast to the classical case of definite causal order which decreases monotonically to zero. Experimentally, we see this increase in information capacity from  $\chi = (2.15 \pm 0.15) \times 10^{-2}$  bits at  $q = 0.78$ , i.e. at its worst absolute performance it is  $13.5 \sigma$  above the classical performance at that value of  $q$ .

To understand this behaviour, consider that for low depolarisation strengths, the minimum entropy  $H^{\min}(\mathfrak{s}[\mathcal{N}^q, \mathcal{M}^q])$  increases more rapidly than the von Neumann entropy  $H(\tilde{\rho}_c)$ . This means that for low  $q$ , the rate of depolarisation of the composite system—target and control—is faster than the rate of depolarisation of the control qubit. However, around  $q = 0.7778$ ,  $H(\tilde{\rho}_c)$  begins to increase more rapidly than  $H^{\min}(\mathfrak{s}[\mathcal{N}^q, \mathcal{M}^q])$  so the depolarisation rate of the control overtakes the depolarisation rate of the composite system, and the information revival occurs.

Quantum mechanics allows indefinite causal order, allowing us to send information through two full strength depolarising channels. In protocols like ours, where the target qubit is the transverse spatial mode, an atmospheric channel can be treated as a generalised Pauli

channel [13]. This opens up new possibilities for communicating through strong atmospheric turbulence using quantum channels. Note that a depolarising channel is just one type of a noisy channel, raising the question as to what other types of noisy channels—if any—can give an advantage with indefinite causal order: in the supplementary material we show that there is no advantage in using a pure amplitude or phase damping channel.

Our quantum switch realises indefinite ordering of only two operations. The most general quantum switch can be extended to arbitrary number of operations [14]. Extending to systems with qudit control will allow exploration of how information theoretic advantage scales up for  $n$ -copies of depolarising channels in a quantum  $n$ -switch. The other scenario known to increase the capacity of a channel is when communicating parties share an entangled resource. The enhancement in this case

is also greatest for very noisy channels [15]. This suggests a future direction exploring similarities between indefinite causal order and entanglement as resources. [16, 17] *Acknowledgements.* This work has been supported by: the Australian Research Council (ARC) by Centre of Excellence for Engineered Quantum Systems (EQUS, CE170100009), a DECRA grant (DE160100409) and L’oreal-UNESCO FWIS grant for JR; the University of Queensland by a Vice-Chancellor’s Senior Research and Teaching Fellowship for AGW; and the John Templeton Foundation (the opinions expressed in this publication are those of the authors and do not necessarily reflect the views of the John Templeton Foundation). We acknowledge the traditional owners of the land on which the University of Queensland is situated, the Turrbal and Jagera people.

- 
- [1] C. H. Bennet and G. Brassard, Proc. of IEEE Int. Conf. on Comp., Syst. and Signal Proc., Bangalore, India, Dec. 10-12, 1984 (1984).
- [2] C. H. Bennet and P. Shor, IEEE Trans. Inf. Theory **44**, 2724 (1998).
- [3] M. Nielsen and I. Chuang, *Quantum Computation and Quantum Information* (Cambridge University Press, 2000).
- [4] M. M. Wilde, Cambridge University Press (2013).
- [5] G. Chiribella, G. M. D’Ariano, P. Perinotti, and B. Valiron, Phys. Rev. A **88**, 022318 (2013), arXiv:0912.0195 [quant-ph].
- [6] O. Oreshkov, F. Costa, and Č. Brukner, Nat. Commun. **3**, 1092 (2012), arXiv:1105.4464 [quant-ph].
- [7] G. Rubino, L. A. Rozema, A. Feix, M. Araújo, J. M. Zeuner, L. M. Procopio, Č. Brukner, and P. Walther, Science Advances **3**, e1602589 (2017).
- [8] K. Goswami, C. Giarmatzi, M. Kewming, F. Costa, C. Branciard, J. Romero, and A. G. White, arXiv:1803.04302 (2018).
- [9] D. Ebler, S. Salek, and G. Chiribella, Phys. Rev. Lett. **120**, 120502 (2018).
- [10] L. M. Procopio, A. Moqanaki, M. Araújo, F. Costa, I. Alonso Calafell, E. G. Dowd, D. R. Hamel, L. A. Rozema, Č. Brukner, and P. Walther, Nature Communications **6**, 7913 (2015).
- [11] A. Holevo, Jour. Problems Inform. Transmission **9**, 177 (1973).
- [12] G. G. Stokes, Trans. Cambridge Philos. Soc **9**, 399 (1852).
- [13] Y. Zhang, I. B. Djordjevic, and X. Gao, Opt. Lett. **37**, 3267 (2012).
- [14] M. Araújo, F. Costa, and Č. Brukner, Phys. Rev. Lett. **113**, 250402 (2014), arXiv:1401.8127 [quant-ph].
- [15] A. Chiuri, S. Giacomini, C. Macchiavello, and P. Mataloni, Phys. Rev. A **87**, 022333 (2013).
- [16] S. Milz, F. A. Pollock, T. P. Le, G. Chiribella, and K. Modi, New Journal of Physics **20**, 033033 (2018).
- [17] S. Akibue, M. Owari, G. Kato, and M. Murao, Phys. Rev. A **96**, 062331 (2017).
- [18] J. Leach, J. Courtial, K. Skeldon, S. M. Barnett, S. Franke-Arnold, and M. J. Padgett, Phys. Rev. Lett.

**92**, 013601 (2004).

SUPPLEMENTARY MATERIAL

**Experimental details.** Our experimental setup is a modified form of the quantum switch of Ref. [8], removing cylindrical lenses and using only inverting prisms, since only Pauli operations where necessary, Fig. 4. Our input light is diagonally-polarised ( $|\rho_c\rangle=(|0\rangle+|1\rangle)/\sqrt{2}=D$ ), and is in the lowest-order vertical-banded spatial mode ( $|\rho_t\rangle=|1\rangle=|\text{HG}_{10}\rangle$ ).

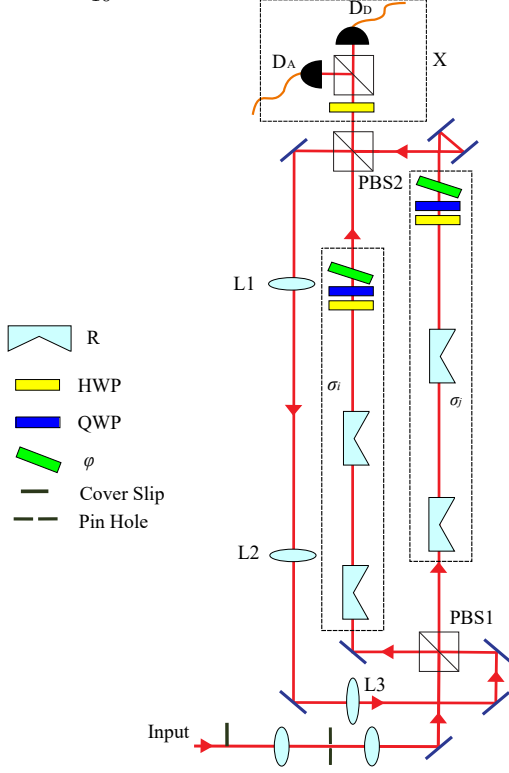


FIG. 4. Schematic of quantum switch. The control qubit is the polarisation,  $|\rho_c\rangle=D$ . The polarisation of the light controls order of Pauli operations  $\{\sigma_i\}$  acting on the photonic spatial mode  $|\rho_t\rangle=|\text{HG}_{10}\rangle$ , for horizontal polarisation  $H$ , the order is  $\sigma_i\circ\sigma_j$ , for the vertical polarisation  $V$  the order is  $\sigma_j\circ\sigma_i$ . The polarisation  $|D\rangle$  ensures superposition of the orders.  $X$  is a polarisation measurement, determining the Stokes parameter of the measured photon in the diagonal/anti-diagonal basis. Lenses L1–L3 form a telescope for mode-matching.

We realise the unitary operations  $\{\sigma_i\}$  using a pair of inverting prisms [18] as shown in Fig. 4. A mechanical rotation of the inverting prism results in a rotation of the incoming spatial mode of the photon, the outputs of the combined operation  $\{\sigma_i\circ\sigma_j\}$  are shown in Figure 2.

To implement  $\sigma_i, \sigma_j$ , we use up to two M-shaped inverting prisms [8] in each arm. Each prism is oriented at a physical angle  $\theta$ , which reflects and rotates an incoming beam by  $2\theta$ . The action of the rotating prism on our target qubit subspace is represented by the following unitary operation:

$$R(\theta) = \begin{pmatrix} -\cos 2\theta & \sin 2\theta \\ \sin 2\theta & \cos 2\theta \end{pmatrix}. \quad (7)$$

Unitary	$\varphi$	$\theta_1$	$\theta_2$
$\sigma_0$	0	$\frac{\pi}{2}$	$\frac{\pi}{2}$
$\sigma_1$	0	$\frac{\pi}{4}$	—
$\sigma_2$	$\frac{\pi}{2}$	$\frac{\pi}{2}$	$\frac{\pi}{4}$
$\sigma_3$	0	$\frac{\pi}{2}$	—

TABLE II. Phases and angles for the unitary operations realised in our experiment, given by Eq. (8).

We impart the global phase  $\varphi$  by a tilted phase plate. We write the transformation performed by the pair of prisms and the phase plate as:

$$U(\varphi, \theta_1, \theta_2) = e^{i\varphi} R(\theta_2) R(\theta_1). \quad (8)$$

We place the phase plate only when we are doing  $\sigma_2$  operation. For operations,  $\sigma_1$  and  $\sigma_3$  we need only one rotating prism, and for  $\sigma_0$  and  $\sigma_2$  we need both prisms. We achieve this by moving the second rotating prism via a translation stage. Table II are the angles and phases used to implement the Pauli operations.

**Quantum switch and amplitude damping.** For a single qubit, the Kraus operators of an amplitude damping channel  $\mathcal{A}$  are given by,

$$A_0 = \begin{pmatrix} 1 & 0 \\ 0 & \sqrt{1-\gamma} \end{pmatrix}, \quad A_1 = \begin{pmatrix} 0 & \sqrt{\gamma} \\ 0 & 0 \end{pmatrix}, \quad (9)$$

where  $\gamma$  denotes the strength of the amplitude damping.  $\gamma = 1$  means a complete damping, in such case action of an amplitude damping on an input state  $\rho$  kills all the components of  $\rho$  and the state becomes  $\rho \rightarrow \mathcal{A}(\rho) = |0\rangle\langle 0|$ .

If two identical amplitude damping channels act in a quantum switch, the resulting channel has Kraus operators given by,

$$S_{ij} = |0\rangle\langle 0|_c \otimes A_i A_j + |1\rangle\langle 1|_c \otimes A_j A_i, \quad (10)$$

$|0\rangle\langle 0|_c$  and  $|1\rangle\langle 1|_c$  are the control qubit states. Here,  $i, j \in \{0, 1\}$ . For an input control state  $|\rho_c\rangle = \sqrt{p}|0\rangle + \sqrt{1-p}|1\rangle$  and target state  $\rho_t = \{\{\rho_{00}, \rho_{01}\}, \{\rho_{10}, \rho_{11}\}\}$ , the action of the quantum switch with amplitude damping is given by,

$$\mathfrak{s}[\mathcal{A}^\gamma, \mathcal{A}^\gamma](\rho_c \otimes \rho_t) = \sum_{i,j} S_{ij} (\rho_c \otimes \rho_t) S_{ij}^\dagger. \quad (11)$$

Tracing out the control state of the output in an arbitrary measurement basis  $|M_c\rangle = \cos \theta |0\rangle + e^{i\phi} \sin \theta |1\rangle$  results in the output target state  $\tilde{\rho}_t = \{\{\tilde{\rho}_{00}, \tilde{\rho}_{01}\}, \{\tilde{\rho}_{10}, \tilde{\rho}_{11}\}\}$ ,

with,

$$\begin{aligned}
\tilde{\rho}_{00} &= \rho_{00}(p \cos^2 \theta + (1-p) \sin^2 \theta \\
&\quad + \sqrt{p(1-p)} \cos \phi \sin 2\theta) \\
&\quad + \rho_{11}\gamma((2-\gamma)p \cos^2 \theta + (2-\gamma)(1-p) \sin^2 \theta \\
&\quad + 2\sqrt{1-\gamma}\sqrt{p(1-p)} \cos \phi \sin 2\theta) \\
\tilde{\rho}_{01} &= \rho_{01}(1-\gamma)(p \cos^2 \theta + (1-p) \sin^2 \theta \\
&\quad + \sqrt{p(1-p)} \cos \phi \sin 2\theta) \\
\tilde{\rho}_{10} &= \rho_{10}(1-\gamma)(p \cos^2 \theta + (1-p) \sin^2 \theta \\
&\quad + \sqrt{p(1-p)} \cos \phi \sin 2\theta) \\
\tilde{\rho}_{11} &= \rho_{11}(1-\gamma)^2(p \cos^2 \theta + (1-p) \sin^2 \theta \\
&\quad + \sqrt{p(1-p)} \cos \phi \sin 2\theta). \tag{12}
\end{aligned}$$

From the equation (12), and taking into consideration  $\rho_{00} + \rho_{11} = 1$ , we observe at the full strength amplitude damping case,  $\gamma = 1$ , the resulting output target state becomes,

$$\begin{aligned}
\tilde{\rho}_t &= \left( p \cos^2 \theta + (1-p) \sin^2 \theta \right. \\
&\quad \left. + \rho_{00} \sqrt{p(1-p)} \cos \phi \sin 2\theta \right) |0\rangle\langle 0|. \tag{13}
\end{aligned}$$

From the equation (13), we can see that even in presence of indefinite causal order we are unable to retrieve information of the input state  $\rho_t$ .

**Quantum switch and phase damping** Kraus operators for a phase damping channel in case of a single qubit are given by,

$$\begin{aligned}
P_0 &= \sqrt{1-\Phi} \begin{pmatrix} 1 & 0 \\ 0 & 1 \end{pmatrix}, \quad P_1 = \sqrt{\Phi} \begin{pmatrix} 1 & 0 \\ 0 & 0 \end{pmatrix}, \\
P_2 &= \sqrt{\Phi} \begin{pmatrix} 0 & 0 \\ 0 & 1 \end{pmatrix}. \tag{14}
\end{aligned}$$

The parameter  $\Phi$ , varying from 0 to 1, denotes the strength of phase damping, with a complete phase damping at  $\Phi = 1$ . In case of a complete phase damping an input state  $\rho$  is transformed into  $\mathcal{P}(\rho) = \langle 0|\rho|0\rangle |0\rangle\langle 0|$ . When two such phase damping channels are used in a quantum switch, the resulting Kraus operators of the overall channel become,

$$S_{ij} = |0\rangle\langle 0|_c \otimes P_i P_j + |1\rangle\langle 1|_c \otimes P_j P_i \tag{15}$$

For the input control and target states as defined in case of amplitude damping, the output of the quantum switch  $\mathfrak{s}(\mathcal{P}^\Phi, \mathcal{P}^\Phi)(\rho_c \otimes \rho_t)$  takes a form similar to the equation (11). Tracing out the control with an arbitrary measurement basis  $|M_c\rangle$  in the control state, as defined in the previous section, the resulting output target state  $\tilde{\rho}_t$  takes the form:

$$\begin{aligned}
\tilde{\rho}_{00} &= \rho_{00}(p \cos^2 \theta + (1-p) \sin^2 \theta \\
&\quad + \sqrt{p(1-p)} \cos \phi \sin 2\theta) \\
\tilde{\rho}_{01} &= \rho_{01}(1-\phi)^2(p \cos^2 \theta + (1-p) \sin^2 \theta \\
&\quad + \sqrt{p(1-p)} \cos \phi \sin 2\theta) \\
\tilde{\rho}_{10} &= \rho_{10}(1-\phi)^2(p \cos^2 \theta + (1-p) \sin^2 \theta \\
&\quad + \sqrt{p(1-p)} \cos \phi \sin 2\theta) \\
\tilde{\rho}_{11} &= \rho_{11}(p \cos^2 \theta + (1-p) \sin^2 \theta \\
&\quad + \sqrt{p(1-p)} \cos \phi \sin 2\theta) \tag{16}
\end{aligned}$$

In case of full phase damping  $\Phi = 1$ , the output target state reduces to

$$\begin{aligned}
\tilde{\rho}_t &= \left( p \cos^2 \theta + (1-p) \sin^2 \theta \right. \\
&\quad \left. + \sqrt{p(1-p)} \cos \phi \sin 2\theta \right) \begin{pmatrix} \rho_{00} & 0 \\ 0 & \rho_{11} \end{pmatrix} \tag{17}
\end{aligned}$$

From the equation (17), we can see the off diagonal elements of the target state is completely vanishes under action of phase damping channels even with the assistance of indefinite causal order.